Human eyelid meibomian glands and tarsal muscle are recognized by autoantibodies from patients affected by a new variant of endemic pemphigus foliaceus in El-Bagre, Colombia, South America

Ana Maria Abreu-Velez, MD, PhD,[a] Michael S. Howard, MD,[a] Takashi Hashimoto, MD,[b] and Hans E. Grossniklaus, MD[c]
Atlanta, Georgia, and Kurume, Japan

Background: Previously, we described a new variant of endemic pemphigus foliaceus (EPF) in Colombia, South America (El Bagre-EPF).

Objective: Continuing our characterization of this variant of EPF, we now focus on one of our previously reported clinical findings: the presence of ocular lesions. These ocular lesions are seen in patients having extensive skin involvement, as measured by the Lund and Browder scale, which is generally used for patients with skin burns.

Methods: We specifically searched for evidence of autoreactivity to various eyelid structures in these patients and correlated our immunologic data with the clinical findings. We performed indirect immunofluorescence studies using normal-appearing human eyelid skin from routine blepharoplasties as substrate tissue. We tested sera from 12 patients with El Bagre-EPF and ocular lesions, 5 patients with sporadic (nonendemic) pemphigus foliaceus, and 20 healthy control subjects (10 from the El Bagre-EPF endemic area and 10 from nonendemic areas). We used fluorescein isothiocyanate conjugated goat antiserum to human total IgG/IgA/IgM as a secondary antibody. In addition, we used fluorescein isothiocyanate conjugated antibodies to human fibrinogen, albumin, IgG, IgE, C1q, and C3, Texas Red (Rockland Immunochemicals, Inc, Gilbertsville, PA), Alexa Fluor 555, or Alexa Fluor 594 (Invitrogen, Carlsbad, CA). Ki-67 (a cell proliferation marker) was used to determine the cell proliferation rate, and nuclear counterstaining was performed with either 4′, 6-diamidino-2-phenylindole or Topro III (Invitrogen, Carlsbad, CA).

Results: We observed autoreactivity to multiple eyelid structures, including meibomian glands and tarsal muscle bundles at different levels, and some areas of the epidermis and the dermis close to the isthmus of the eyelids. Tarsal plate autoreactivity was seen in 10 of 12 of the El Bagre-EPF sera and in one control with pemphigus erythematosus. Furthermore, immunoprecipitation using an eyelid sample as a substrate with 1 mmol/L of sodium orthovanodate showed autoreactivity to several antigens, including some of possible lipid origin.

Limitations: The main limitation of this study is the fact that the antigen or antigens remain unknown.

Conclusion: We identified for the first time to our knowledge autoantibodies to meibomian glands and tarsal muscle in El Bagre-EPF. Our findings suggest that the autoantibodies to the ocular structures cause

From Georgia Dermatopathology Associates[a]; Department of Dermatology, Kurume University School of Medicine[b]; and Department of Ophthalmology, Emory University Medical Center, Atlanta.[c]

Supported by Georgia Dermatopathology Associates (Dr Howard). The El Bagre-endemic pemphigus foliaceus samples were collected with the support of previous grants from the Embassy of Japan in Bogota, Colombia, (Dirección Seccional de Salud de Antioquia), U. de A, Mineros SA (anonymous society) (SA) (Dr Abreu-Velez), Medellin, Colombia, South America, and Emory University Medical Center (Dr Grossniklaus). Our studies were also funded by a Grant-in-Aid for Scientific Research from the Ministry of Education, Culture, Sports, Science and Technology of Japan, and by a grant from the Ministry of Health, Labor and Welfare (Research on Intractable Diseases [Dr Hashimoto]).
Conflicts of interest: None declared.
Accepted for publication June 3, 2009.

Reprint requests: Ana Maria Abreu-Velez, MD, PhD, Georgia Dermatopathology Associates, 1534 N Decatur Rd NE, Suite 206, Atlanta, GA 30307-1000. E-mail: abreuvelez@yahoo.com.

Published online January 11, 2010.
0190-9622/$36.00

doi:10.1016/j.jaad.2009.06.007

the clinical and histopathological findings in the ocular lesions in El Bagre-EPF. (J Am Acad Dermatol 2010;62:437-47.)

Key words: autoimmunity; endemic pemphigus foliaceus; meibomian glands; tarsal muscle.

Endemic pemphigus foliaceus (EPF) is an autoimmune disease occurring in specific geographic foci, mostly in South America. Thus, this disorder represents an interesting model to study how the environment, individual genetics, and immunologic factors can influence autoimmune disease.[1-4] We have previously reported a new variant of EPF (El Bagre-EPF) in El Bagre and surrounding rural mining municipalities in Colombia, South America, and compared it with its Brazilian counterpart, fogo selvagem (FS).[5,6] The El Bagre-EPF variant resembles Senear-Usher syndrome (pemphigus erythematosus [PE] or seborrheic pemphigus), and differs from other types of pemphigus in many respects.[5,6] The primary disease antigens in FS are desmogleins (Dsgs), proteins; recently, E-cadherin was also shown to be an antigen.[7] In El Bagre-EPF, in addition to Dsg1, plakin family proteins and other unknown antigens have been detected.[5,6] Based on our previous clinical studies, we noted ocular alterations in patients with El Bagre-EPF and significant skin involvement, as measured by the Lund and Browder scale used for patients with burn.[8] As a result of the preceding concepts and the predominant seborrheic presentation of this disease, we investigated autoimmune reactivity to eyelid components in these patients.

CAPSULE SUMMARY

- We demonstrate that patients with extensive El Bagre-EPF may have involvement of several ocular structures.
- We describe autoantibodies to meibomian glands and tarsal muscle in this form of endemic pemphigus.
- Ocular examination should be performed routinely in all patients with pemphigus.

METHODS

We randomly tested 12 sera from patients with El Bagre-EPF who fulfilled clinical, epidemiologic, and immunologic criteria for this disease, and who showed ocular lesions including conjunctivitis-like changes.[5,6,9] Five sera from patients with sporadic pemphigus foliaceus (PF) and 20 sera from healthy control subjects (10 from the El Bagre-EPF endemic area and 10 from nonendemic areas) underwent specific immunologic characterization by indirect immunofluorescence (IF), immunoblotting (IB), and immunoprecipitation (IP) as previously described.[9] Indirect IF and IP were conducted as described previously,[9] with some modifications to evaluate tissues rich in lipids (ie, the rationale for possible antigens that could be lipid-associated molecules including lipoproteins). For this purpose, we added 1 mmol/L of sodium orthovanodate to the eyelid extracts for IP. All samples were tested anonymously to comply with institutional review board requirements. Table I summarizes the results in all El Bagre-EPF sera.

Indirect IF

We obtained eyelid skin samples from aesthetic reductions in Michel medium (Newcomer Supply, Middleton, WI). We created 4 μm–thick cryostat-cut sections and partially fixed them in paraformaldehyde in phophate-buffered saline (PBS). The slides were then rinsed, partial solubilized in PBS-0.5% Triton X-100 pH 6.8 buffer (Roche Applied Science, Mannheim, Germany), and rinsed again in PBS. Next, the samples were incubated with the sera at 1:20 and 1:40 dilutions in PBS-0.05% Triton. Then, the samples were rinsed twice in PBS and incubated again with secondary antibody cocktails diluted in PBS (goat antihuman total IgG/IgA/IgM– fluorescein isothiocyanate [FITC] conjugated) (Zymed, Invitrogen, Carlsbad, CA). In addition, other slides were incubated with other secondary antibodies: FITC-conjugated rabbit antisera to human fibrinogen, albumin, IgA, IgG, and C3 (DakoCytomation, Carpinteria, CA).

Based on the rationale that the eyelid and the tear film barrier are constantly reformed and replenished, we also used rabbit antihuman IgG conjugated with Alexa 488 (Invitrogen) to see whether the continued cell-renewal process could be affected in this autoimmune disease. After these incubations, the slides were rinsed twice in PBS again, and were incubated with an anti-Ki-67 antigen mouse monoclonal antibody at 1:50 dilution (IgG1, immunogen: recombinant protein representing a 1086–base pair Ki-67 motif-containing complementary DNA fragment) (Vector Laboratories, Inc, Burlingame, CA). Ki-67 is

Abbreviations used:

BMZ: basement membrane zone
Dsg: desmoglein
EPF: endemic pemphigus foliaceus
FITC: fluorescein isothiocyanate
FS: fogo selvagem
IB: immunoblotting
IC: intercellular
IF: immunofluorescence
IP: immunoprecipitation
PBS: phophate-buffered saline
PE: pemphigus erythematosus
PF: pemphigus foliaceus
SDS: sodium dodecyl sulfate

a cell proliferation marker, and our Ki-67 antibody cross-reacts with human, rat, and mouse Ki-67. The slides were washed, and then incubated with a secondary antibody for Ki-67, donkey antimouse IgG (heavy and light), at a 1:100 dilution (Jackson Immuno Research Labs, Jackson, ME). Finally, the slides were counterstained either with DAPI (Pierce, Rockford, IL) or Topro III (Invitrogen), washed, coverslipped, and dried overnight at 4°C.

A second set of experiments was performed using conventional, paraffin-embedded skin samples fixed in 10% buffered formalin, initially processed in the L.F. Montgomery Eye Pathology Laboratory of the Department of Ophthalmology at Emory University Medical Center, Atlanta, GA. For this experiment, we developed our own protocol using paraffin-embedded skin slides cut at 4 μm. For antigen retrieval, the sections were incubated at 60°C for 40 minutes to remove excess paraffin. Then, with cotton-tipped swabs, paraffin was manually removed. This procedure was repeated twice at exactly the same oven temperature. The tissues were rinsed twice with extraction buffer (PBS with 0.5% Tween [Sigma-Aldrich, St Louis MO]) at 37°C for a few minutes. The first antibodies (patient and control sera) were added at the same dilution using the extraction buffer, but in this case the incubation was set overnight at 4°C. For secondary antibodies, in addition to those outlined above, we used rabbit antihuman IgG antiserum conjugated with either Alexa Fluor 555 or Alexa Fluor 594 (Invitrogen). Finally, all sections were observed with a microscope (Eclipse 50i, Nikon, Tokyo, Japan) using a Xenon arc light (XBO 75 W) as the light source and a PL APO ×40/0.80 dry objective. The slides were visualized using both a FITC filter and a triple filter (Nikon) (DAPI [Pierce]/FITC/Texas red triple EX 395-410/490-505/560-585, EM 450-490/515-545/600-652). Simultaneously to the IF evaluations, a quick hematoxylin-eosin stain was performed for each case to evaluate the quality of the tissue used as the antigen source.

IP and IB procedures

The sera were evaluated by sodium dodecyl sulfate (SDS)-polyacrylamide gel electrophoresis using iodine-125-labeled 48-kd tryptic fragments of Dsg1 purified by Concanavalin A affinity chromatography as described previously.[5,6,9] We also performed IB using human whole eyelid skin samples, which were extracted in 62.5 mmol/L Tris-HCl buffer (pH 6.0) containing 0.8 mol/L of orthovanodate (Mallinckrodt Baker, Inc, Phillpsburg, NJ).[10] To detect possible lipid antigens we used a lysis buffer containing a protease inhibitor cocktail (Roche Molecular Biochemicals, Mannheim, Germany) and 1 mmol/L of sodium orthovanodate. In brief, SDS extractions were performed using eyelids rinsed with ice-cold Tris buffered saline (TBS), pH 8.0. The meibomian glands and adjacent tissues were scraped and lysed in 0.1% SDS in TBS with 2 mmol/L of phenylmethylsulphonyl fluoride, 20 mmol/L of sodium fluoride, 10 mmol/L of sodium pyrophosphate, a protease inhibitor cocktail (Roche Molecular Biochemicals), and 0.8 mol/L of sodium orthovanadate. An equal volume from each sample was centrifuged at 1000*g* for approximately 30 minutes at 4°C. After adding 1% SDS in TBS with phosphatase inhibitors to the low-speed pellets, the mixture was boiled with intermittent vortexing.[10] Protein concentrations were determined using a DC protein assay kit (Bio-Rad DC Protein Assay Kit I, Hercules, CA) and the protein content of homogenates was adjusted to equal concentrations. Equal amounts of protein were resolved using NuPage 4% to 12% Bis-Tris gels (Invitrogen) and identified by IB on PVDF membranes (Invitrogen). Molecular weight standards were used in each gel (Invitrogen). We used horseradish peroxidase-conjugated antitotal human IgG/IgA/IgM antiserum (Southern Biotechnology, Birmingham, AL). The blots were examined using chemiluminescence (Western Lightning Chemiluminescence, PerkinElmer Life Sciences Inc) and exposed to radiographic film (Kodak, Rochester, NY). To show the results of the IB, preincubation was performed for 1 hour at room temperature in 5% nonfat dry milk, 0.05% Tween-20 in 10 mmol/L of Tris-HCl, 154 mmol/L NaCl, pH 7.5.[10] Then, the membranes were washed twice for 10 minutes with PBS-Tween-20, and then incubated with the first antibody (either patient or control sera), diluted at 1:75 dilution in 1% bovine serum albumin/PBS-Tween-20, and incubated for 2 hours. The membranes were then washed several times with PBS-Tween-20 for 15 minutes. Next, the membranes

Table I. Summary of laboratory findings and common ocular findings in El Bagre-endemic pemphigus foliaceus

Sex	DX	DIF IgG1	DIF IgG total	IIF IgG4	IB-160	IP 45, 200, 117, 89, 34	Red eye	Clinical entropion and/or ectropion, trichiasis, blepharophimosis, thinned eyebrows
F	El Bagre-EPF 1	(−)	(+++)	(++)	(++)	(+++)	(+++)	(+++)
M	El Bagre-EPF 2	(−)	(++)	(++)	(1/2 +)	(++)	(++)	(++)
F	El Bagre-EPF 3	(−)	(+++)	(+++)	(++)	(+++)	(++)	(++)
M	El Bagre-EPF 4	(−)	(−)	(+)	(−)	(1/2 +)	(+++)	(+++)
M	El Bagre-EPF 5	(−)	(+)	(++)	(1/2 +)	(+)	(+)	(+)
M	El Bagre-EPF 6	(−)	(++)	(+++)	(−)	(++)	(++)	(++)
M	El Bagre-EPF 7	(−)	(++)	(++)	(+++)	(+++)	(+++)	(+++)
M	El Bagre-EPF 8	(−)	(++)	(+++)	(++)	(++++)	(−)	(−)
M	El Bagre-EPF 9	(−)	(++)	(+++)	(++)	(++++)	(++++)	(++++)
M	El Bagre-EPF 10	(−)	(++)	(++)	(−)	(++)	(++)	(++)
M	El Bagre-EPF 11	(−)	(++)	(++)	(+++)	(+++)	(+++)	(+++)
M	El Bagre-EPF 12	(−)	(++)	(+++)	(−)	(++)	(+++)	(+++)
M	PE	(−)	(++)	(+++)	(−)	(++)	(++)	(++)
M	PF 1	(−)	(−)	(+++)	(++)	(45 Only)	(+)	(+)
M	PF 2	(−)	(−)	(+++)	(++)	(200, 45, 34)	(++)	(++)
M	NHS 1	(−)	(−)	(−)	(−)	(−)	(−)	(−)
M	NHS 2	(−)	(−)	(−)	(−)	(−)	(−)	(−)

DIF, Direct immunofluorescence; *DX*, diagnosis; *EPF*, endemic pemphigus foliaceus; *F*, female; *IB*, immunoblotting; *IIF*, indirect immunofluorescence; *IP*, immunoprecipitation; *M*, male; *NHS*, normal human serum; *PE*, pemphigus erythematosus; *PF*, pemphigus foliaceus.

were incubated with horseradish peroxidase-labeled secondary antibodies, diluted in 1% bovine serum albumin/PBS-Tween-20, and then incubated with the membranes for 90 minutes. Finally, we washed the membranes several times with PBS-Tween-20. After this, we prepared the chemiluminescence reagent (0.125 mL of chemiluminescence reagent/cm^2 of membrane) by mixing equal volumes of the enhanced luminol reagent and the oxidizing reagent, and incubated the membrane in the chemiluminescence reagent for 1 to 3 minutes with shaking. The reaction was stopped when the proteins were visualized.[10]

Ophthalmic clinical evaluation

Ophthalmic clinical evaluations were performed in an El Bagre local hospital by two residents of the Department of Ophthalmology from the Institute of Health Sciences (Instituto de Ciencias de la Salud) in Medellin, Colombia.

RESULTS

Clinical findings

In Table I, we compare major ocular involvement and laboratory findings for the most significant subjects of the study. In Fig 1, we show several pictures revealing ocular area lesions in patients affected by El Bagre-EPF. Our most common clinical findings included: (1) 10 of 12 patients showed meibomianitis and partial occlusion of the meibomian ducts, pingueculae, amblyopia, refractory defects, chalazia, superior tarsal muscle edema or hypertrophy (in the acute stages, likely a consequence of the inflammatory process), red eye, nasal ptyrigia, and melanosis; (2) all 12 patients experienced a sensation of a foreign body in the eye; (3) 3 of 12 patients displayed open angle glaucoma; and (4) 11 of 12 patients displayed cortical-nuclear cataracts. In several cases, bilateral severe swelling, induration, and thickening of eyelids, as well as some conjunctival and lid margin erosions, were appreciated. Fig 1, *A*, *C*, and *D*, show lesions of the palpebral skin, which could indirectly affect eyelid motility (Ameondola).[11] The palpebral skin is one of the most delicate structures of the human body. Small undetected blisters or inflammation, especially in exfoliative form, may result in fibrosis; this process could alter the palpebral border, and lead to an oblique direction and contraction of the orbicularis muscle, which would in turn drag the free margin of the eyelid backward. As a consequence, some clinical entropion of the upper lids, tylosis, trichiasis, and blepharophimosis could result, and such conditions are indeed shown. The resulting deviation of the eyelashes of the upper eyelid could cause continuous trauma of the anterior corneal surface, and superficial inflammation in this region, with formation of pannus lesions, vascularized loops, and superficial keratitis, all of which cause severe visual disturbances. The illustrations show rarefaction of the eyebrows, blepharoptosis, blepharophimosis, decrease of the muscular tonus in the

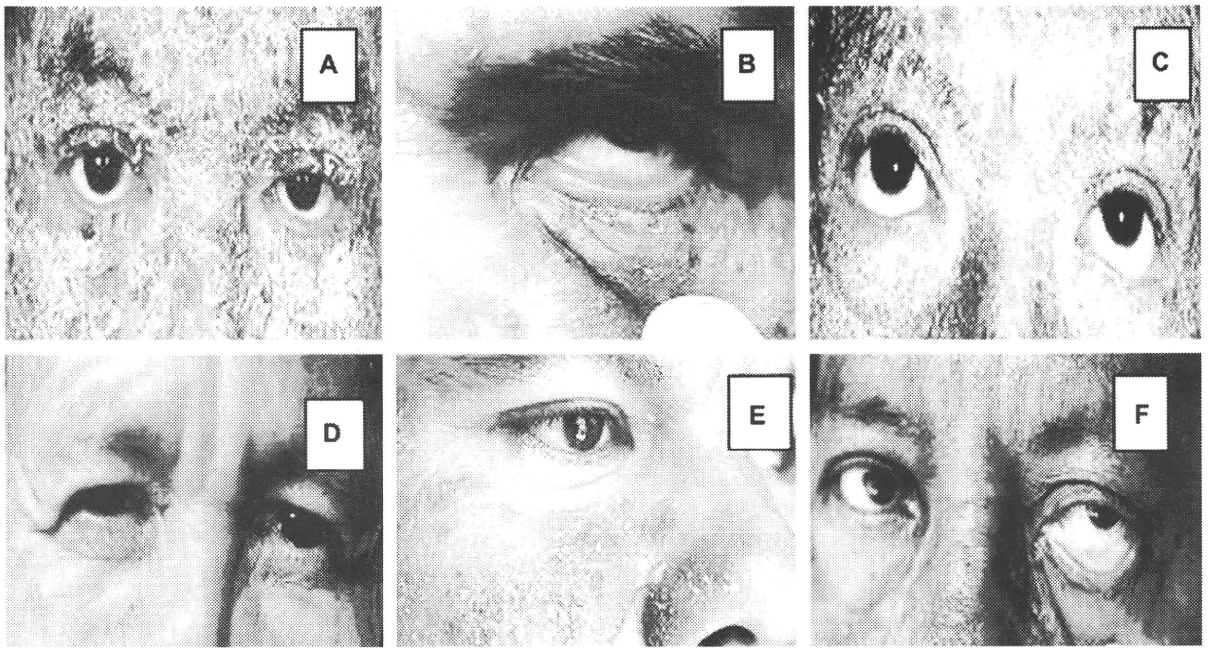

Fig 1. Clinical images of El Bagre-endemic pemphigus foliaceus (EPF). **A**, Edema, erythema, and scaling of eyelids with severe ectropion. **B**, Hyperemia, edema, erythema, and conjunctival injection without mucoid discharge. **C**, Dry eye and atrophy of superior and inferior tarsal muscles. **D**, Catarrhal conjunctivitis-like alterations characterized by significant edema of superior and inferior eyelids. Small internal synechiae (as rare finding) resembling nasal ptyrigia in internal cantus of left eye. **E**, Most common clinical findings include meibomianitis of lower eyelid and partial occlusion of meibomian ducts. **F** (as in **B**), Hyperemia, edema, erythema, and conjunctival injection, in this case with mucoid discharge. **A, D, C,** and **F,** Thinning of eyebrows.

lower lid, entropion of the upper lid, slight ectropion of the lower lid, perilimbic vascular invasions, and corneal pannus lesions. Descemetocele causes dryness of the epithelium, infiltration of intima, blisters, and possible fusion of the resulting ulcers. In agreement with the description of Ameondola,[11] we found other alterations that included thinned eyebrows, entropion in severe cases, mild blepharophimosis, pseudoptosis, lagophthalmos, muscular atrophy (especially in chronic cases), decreased muscular tone, and inflammation of the tarsal plate (Fig 1). In some cases, descemetocele, perilimbic vascular invasion, corneal pannus lesions, and infiltration of the intima were seen, and in the iris, some diffuse brownish pigmentation with red color was observed as well. Several forms of cataracts were seen, including central opacity in the anterior cortex of the lens, and cortical anterior cataracts, with opaque dots in the entire cortical layer. Intriguingly, the presence of subcapsular cataracts did not differ significantly between the patients and the control subjects. In the control groups of similar age and sex, the main finding was racial melanosis (7/10).

Immunologic findings

In Fig 2, *A*, 5 of 12 patients with El Bagre-EPF and one of 5 patients with PF and higher antibody titers to antihuman IgG4 and/or total IgG showed 9 positive intercellular (IC) staining findings in the conjuctiva. Fig 2, *A*, shows a typical staining seen in a serum from one patient with El Bagre-EPF displaying moderate to bright IC fluorescence among the keratinocytes, and basement membrane zone (BMZ) stain. Control sera consistently revealed negative findings for both of these autoantibody patterns, with the exception of the serum from a seborrheic pemphigus that showed a similar pattern. Fig 2, *C* and *F*, present images for the skin samples that were processed with our antigen retrieval technique. In these cases, we were able to see some reactivity to possible cell junctionlike dots when using antibodies to antihuman fibrinogen and antihuman albumin conjugated with FITC. This reactivity was seen around the meibomian glands and their ductus, around the tarsal muscle bundles, and around the isthmus of the eyelid. This dot immunoreactivity seemed to display two different patterns. The first pattern was fine, dotlike puncta, and was noted

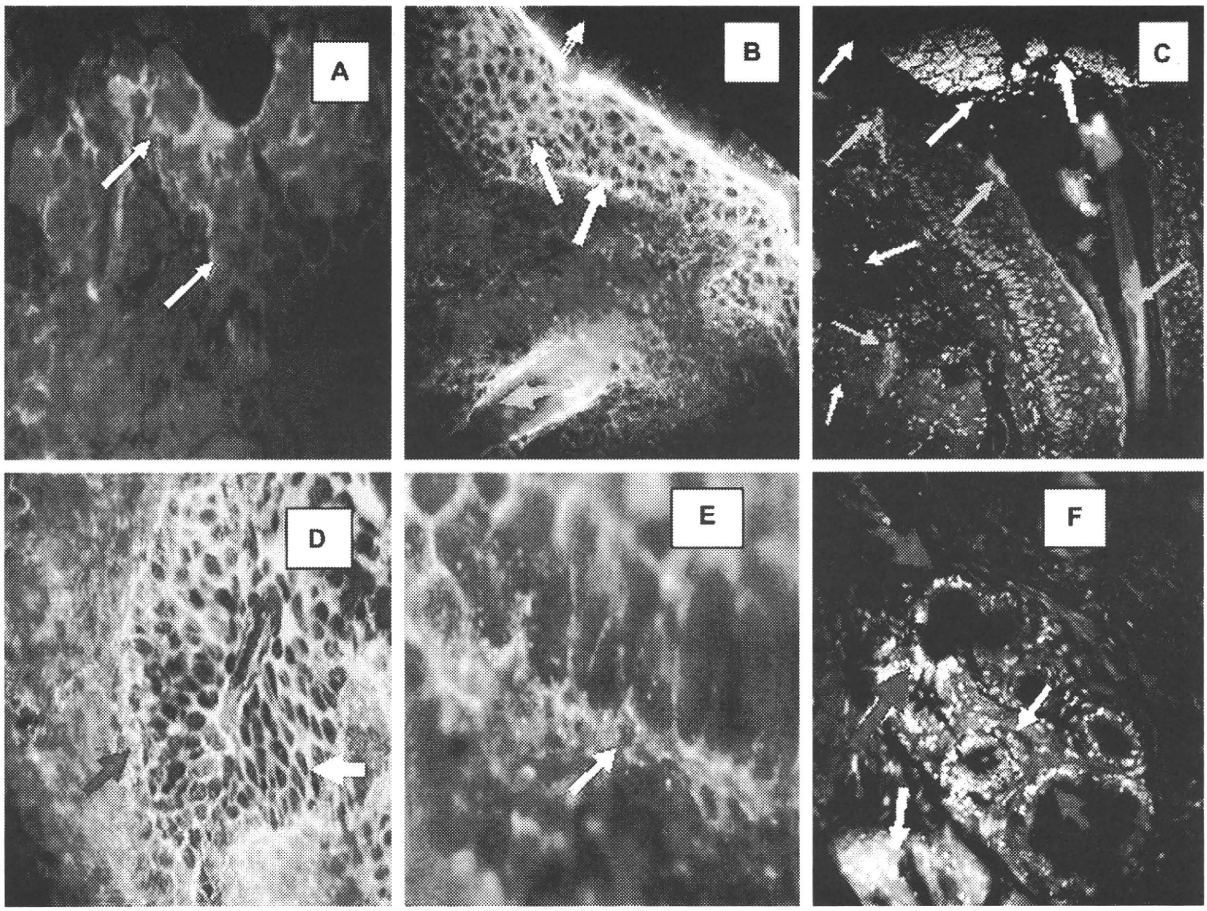

Fig 2. A, B, D, and **E**, Results of indirect IF (IF) performed after partial fixation with paraformaldehyde. **C** and **F**, Results of indirect immunofluorescence performed using paraffin-fixed samples followed by antigen retrieval techniques. **A**, Using conjuctiva as the antigen source, antihuman conjugated IgG-Alexa 488 (Invitrogen) showed positive ICS and basement membrane zone (BMZ) staining (*white arrows*). **B**, Positive intercellular (IC), BMZ, and hair follicle staining using antihuman total IgG antiserum as secondary antibody (*green*) (fluorescein isothiocyanate [FITC]) (*white arrows*). Nuclei of cells were stained with Topro III (Invitrogen) (*red*). In addition, note strong reactivity of hair follicle bulb to Ki-67 proliferating antigen (*red*) (Texas Red) (*blue arrow*). **C**, Structure (*top*) that resembles secretion near tear duct, likely of mixed material including mucins, lipids, and other tear components. These components contribute to high, non-Newtonian viscosity of tear film and its low surface tension, features essential for tear film stability (*white arrows*). In same figure, Ki-67 antigen demonstrated clumped elongated pattern around eyelid base, within isthmus, and in some parts of epidermal layer (*red*) (*green arrows*). Positive autoreactivity as small and large dots (*red*) using Alexa Fluor 555 (Invitrogen) against human IgG (*yellow arrows*). Nuclei were counterstained with DAPI (Pierce) (*blue*). **D** and **F**, IC and BMZ staining were seen in El Bagre-endemic pemphigus foliaceus using antihuman conjugated IgG FITC (*white arrows*) (×20). **D**, BMZ staining of meibomian glands (×100). **E**, Secretory portion of meibomian gland, in yellow dots, as part of intrinsic fluorescence of these structures (*purple arrows*). Ki-67 antigen showed positive clumped pattern surrounding involving base of gland ducts on eyelid (*white arrows*).

along the BMZ and ducts of the meibomian glands, as well as around the epidermis and dermis close to the isthmus of the eyelashes. These dot patterns were also consistently seen around the muscle bundles of the tarsal plates (8 of 12 patients with El Bagre-EPF). No control subjects displayed positive results with this pattern with the exception of one patient with seborrheic pemphigus. The second cell junctionlike dot pattern manifested as larger, irregular, and in some cases clumped dots of reactivity, occurring in

patterns suggesting polarity within underlying cells. This pattern was observed in some diagonal distributions along the meibomian glands, their BMZ (Figs 2, *D* and *E*), ducts, and the tarsal muscle bundles.

In contrast, when we studied the skin samples using the partial fixation of paraformaldehyde (Fig 2, *B*, *D*, and *F*), we were able to see some pattern that reminded us of the IC staining, as seen in pemphigus and along the BMZ of the meibomian glands (×40 and ×20) (Fig 2, *D* to *F*). We were thus able to observe that the prefixation of the samples with paraformaldehyde unmasked a true reactivity, which usually in nonfixed skin samples and nonnucleicounterstained samples is routinely considered to be background. In Fig 2, *B*, *C*, and *F*, we were also able to see 3 types of staining patterns using the antiserum to Ki-67 antigen. One pattern of reactivity was seen in single basal cells inside the meibomian glands in close proximity to the detected patient's autoantibodies (Fig 2, *C*) (large blue arrow). The other pattern was seen as an elongated linear staining around some spots of the mostly eyelid isthmus and in the meibomian ductus (Fig 2, *C*). The final pattern of distribution of Ki-67 was basically exclusive to the secretory part of the ductus of the meibomian glands. This may be related to high levels of cell proliferation.

Fig 3 summarizes how we were able to demonstrate, with laboratory findings, those alterations reported by Ameondola[11] 60 years ago. We were able to demonstrate autoreactivity of the tarsal bundle muscle using eyelid skin as a substrate partially fixed on paraformaldehyde. Consistent with the strong reactivity of tarsal muscle, general muscle atrophy was seen in El Bagre-EPF as described in FS by Ameondola.[11] During the past few years, we have noticed possible autoreactivity in some skeletal muscles, and in light of the positive findings of autoreactivity to tarsal muscle, in addition to the fact that some patients with El Bagre-EPF experience significant muscular weakness and sudden death syndrome, we decided to perform some preliminary studies using skeletal and heart muscle. To test this, we used histoarray tissue microarray slides (frozen sections of various normal human organs; 20 organs in duplicate) (Imgenex, San Diego, CA). In this immunoassay, 10 of 12 patients with El Bagre-EPF had positive findings for antitarsal antibodies, and 7 of 10 displayed antibodies to either skeletal or heart muscle (unpublished data). In testing the heart muscle, we used monoclonal anti-connexin-43 antibody (Clone CXN-6; ascites fluid) (Sigma-Aldrich Co, St Louis, MO) as the first antibody, to search for possible colocalization with patients with El Bagre-EPF. As a secondary antibody for the connexin antibody, we used CY3-conjugated, affinity purified donkey antimouse IgG (heavy and light chain) antiserum (red stain). No control subjects had positive findings for indirect IF. Fig 3 shows a series of experiments demonstrating our results. Of particular interest is the finding that one patient's serum with sporadic PE (or seborrheic pemphigus) from Colombia (not from the endemic area), who displayed 75% skin involvement by the Lund and Browder scale, also showed autoantibodies to meibonian glands and to the tarsal and skeletal muscle, but not to the heart. Fig 3, *I*, shows the results of IP, revealing several antigens that are specifically recognized by the sera from patients with El Bagre-EPF. This image was taken after exposing the membranes to autoradiography film (X-OMAT Blue, Kodak) for 30 seconds. We developed the films by determining an optimum exposure (background vs real bands). Protein bands were quantified by visual examination only, and not with software assistance.

DISCUSSION

Since the initial report by Francis Senear and Barney Usher regarding PE (ie, Senear-Usher syndrome or seborrheic pemphigus), the anatomic predisposition of this disease for seborrheic areas has been well established.[12,13] We have described a new variant of EPF that resembles Senear-Usher syndrome in many aspects.[12,13] In our current study, we compared immunologic alterations in the eyelid with the clinical alterations previously observed in patients with El Bagre-EPF. We previously showed that El Bagre-EPF clinically affected predominately seborrheic areas, and that some patients also displayed a predisposition for axillary lesions. The seborrheic areas include the eyelids with modified sebaceous glands (also known as meibomian glands).[14,15] Recently, a proteomic analysis of human meibomian gland secretions was reported.[16] The analysis demonstrated a complexly large number of heterogeneous molecules, including alpha2-macroglobulin receptor, IgA alpha chain, farnesoid X activated receptor, interferon regulatory factor 3, lacritin precursor, lactotransferrin, lipocalin 1, lysozyme C precursor, potential phospholipid transporting ATPase IK, a transmembrane helix receptor (also termed somatostatin receptor type), and TrkC tyrosine kinase, development-related NYD-SP21 among others.[16] The authors indicated that the meibomian gland secretes a number of proteins into the tear film. It is quite possible that these proteins contribute to the dynamics of the tear film in both healthy and disease conditions. On the other hand, the entire eyelid including the meibomian glands, the tarsal muscle, and the conjunctiva are packed with small

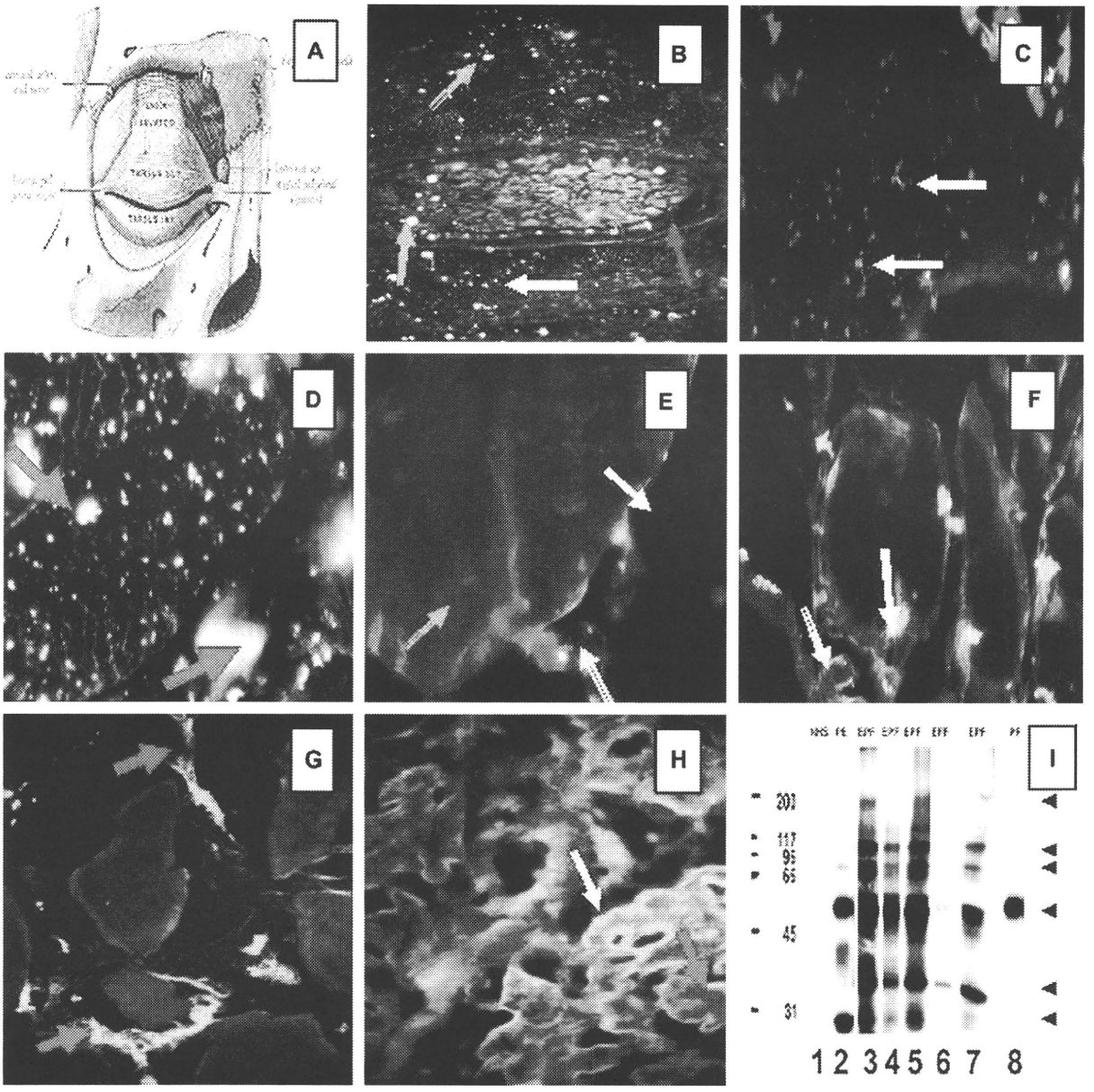

Fig 3. A, A diagram of the eye superior tarsal muscle (musculus tarsalis superior) showing a panoramic view of a tarsal plaque. (Reprinted from Gray H. Gray's Anatomy of the Human Body. 20th ed. Philadelphia: Lea & Febiger;1918.) **B,** Direct IF shows a panoramic view of a tarsal plaque with small continuously yellow-greenish dots around the plaque (*red arrow*). In addition to this, reactivity to larger dots (*blue arrows*) and smaller ones (*white arrow*) was observed. These findings were seen using a secondary goat antihuman IgG/IgA/IgM antiserum conjugated with FITC. **C,** Positive red dots, seen in bundles of tarsal muscle, using antihuman IgG antiserum conjugated with Alexa Fluor 594 (*white arrows*). **D,** Using conjugated antihuman IgG Alexa 488 (*yellow stains dots*), larger bundles of tarsal muscle show positive reactivity of different shapes inside the myocytes (*purple arrows*). In this case, the reactivity was seen with antihuman fibrinogen FITC conjugate. In addition, thin zig-zag yellowish positivity was seen inside the muscle bundles resembling the staining of sarcoplasmic structures. **E,** When repeating the experiments using antihuman fibrinogen FITC conjugate alone, the staining shows a positive reactivity outside the myocytes, as seen at higher magnification (*green staining*) (*blue arrow*). In addition, there is a structure that resembles a "large-cell junction" (*red staining*) (*yellow arrow*) using antihuman IgM antiserum conjugated with rhodamine. The white arrow indicates the extracellular space. **F,** The white arrow shows autoreactivity to a large

blood vessels and are innervated by a fine network of nerves. These nerves are positive to neuron-specific enolase, abundant in smooth and varicose nerve fibers closely apposed to the basement membranes of acini of the meibomian glands. Other neural markers highly expressed in these areas includes the neuropeptide Y and the vasoactive intestinal polypeptide. Nerve fibers and small vessels are also visualized in other eyelid structures, including conjunctiva, epidermis, hair follicles, and subconjunctival and in the lymphoid follicles. We have detected autoantibodies to several nerves and vessels in El Bagre-EPF (Abreu et al, unpublished data).

This study showed for the first time to our knowledge that meibomian gland BMZ and IC junctions seem to be recognized by specific antibodies in patients with El Bagre-EPF and in patients affected by Senear-Usher syndrome. However, the identification of potential antigens is beyond the scope of this article and requires examination. As previously noted, no blisters, scarring, crusts, or pustules have been found clinically on the palms, soles, or oral mucosa of patients with either EPF or sporadic forms of PF (Cazenave pemphigus foliaceus).[17-19] Previous studies have shown expression of pemphigus antigens in the epidermis, and that lack of mucosal involvement in PF may be a result of the low expression of Dsg1.[18,19] This finding may be inconsistent with ours, because the previous authors did not perform prefixation by paraformaldehyde in the direct and indirect IF or IP. Indeed, we clearly showed a specific antigenic response in those patients with El Bagre-EPF that was different from the results of our own previous studies, performed without these prefixation procedures.[8-10]

Anatomically, human palms, soles, and oral mucosa do not contain hair follicles or sebaceous glands. The largest numbers of sebaceous glands, and the largest glands, are located on the face and scalp.[14,20] Sebaceous glands secrete sebum via a very active holocrine mechanism and could be the explanation for the increased expression of Ki-67.[14,20] Significantly, we detected high levels of staining in the BMZ of these glands in patients with El Bagre-EPF and in one sporadic PE control with extensive skin involvement. We also observed different patterns of staining with Ki-67 (a cell proliferation marker), for which the significance and relationship to the pemphigus autoantibodies remain unknown. Thus, we suggest that meibomian gland antigens, including lipids or lipid-associated protein, could be part of this new variant of EPF. Furthermore, these antigens may be present in other types of superficial pemphigus with extensive skin involvement; however, a larger number of samples needs to be tested.

Classically, in pemphigus and bullous pemphigoid, most described antigens are proteins; however, in other diseases, several lipid antigens have been associated with multiple disease processes.[21,22] Indeed, lipid rafts are plasma membrane microdomains that have been implicated in the maintenance of diverse cell signaling pathways, such as those mediated by growth factors, morphogens, integrins, and antigen receptors on immune system cells.[21,22] Even Dsgs are embedded in this large lipid cell membrane-associated structure. It has been also

structure inside the myocytes using antihuman IgG FITC conjugated. The yellow arrow shows autoreactivity to the plasma membrane. **G,** We performed IIF testing on heart muscle tissue from sheep, beef, rat, and human, to determine if the reactivity could be observed in multiple species. Positive staining was noted among the muscle bundles (*green staining*) utilizing FITC conjugated antihuman fibrinogen (*red arrows*). This staining was noted when rabbit antihuman fibrinogen and albumin antisera were used. **H,** We used tissue microarray slides as the antigen source with Alexa 488 conjugated and antihuman IgG heavy and light chain (H&L) antiserum. We again showed positivity within muscle bundles (*green staining*) (*yellow arrow*). To identify colocalization with the autoreactivity detected by antihuman IgG for gap junctions, we used an antibody to connexin-43 as a control (*brown staining*) (*red arrow*). However, the autoreactivity did not superimpose with connexin-43, although confocal microscopy was not performed. (Note that in **D, E, F,** and **H,** the cell nuclei were counterstained with DAPI [blue]). **I,** The sera were tested by IP, and an approximately 45 kDa protein band was strongly recognized by sera with numbers 2, 3, 4, 5, and 7 (and very weakly by number 8). In addition to this band, other antigenic bands were immunoprecipitated, mostly by the El Bagre-EPF patient sera (numbers 2, 3, 4, 5, 7). As a control, we also used normal human serum (NHS) (Lane 1). Lanes 3 to 7 correspond to sera from El Bagre-EPF patients, and lane 8 corresponds to serum from a sporadic PF patient. The molecular weight marker standards are shown in the first lane on the left (200, 117, 96, 66, 45, and 31 kDa, respectively). The arrows on the right point to protein bands of approximately 200, 117, 89, 67 and 34 kDa that were consistently recognized by the El Bagre-EPF sera, and to lesser extent, by the sera from patients with pemphigus erythematosus. Although we show the results of 7 sera, all 12 sera showed similar results.

demonstrated that IgA is secreted by normal human sebaceous and sweat glands. Because it is well known that IgA plays an important role in the inactivation of invading viruses, bacteria, and other antigenic structures on mucous membranes, it appears that IgA in sebum and sweat fulfills a similar function on the outer body surface.[23] In fact, some lipid rafts containing a given set of proteins can change their size and composition in response to intra- or extracellular stimuli,[24] perhaps inducing abnormal activation of signalling cascades. Eyelid skin involvement has also been reported in sporadic PF. Thus, ocular pemphigus is probably underdiagnosed and its frequency appears to be underestimated.[25,26]

Our second finding was the autoreactivity detected by indirect IF to several tarsal plate structures, correlating with the tarsal atrophy and other clinical findings described by Ameondola,[11] who described tarsal muscle ocular findings not only in PF, but also in FS. Several areas of the tarsal muscle were specifically recognized by the autoantibodies in the sera of patients with El Bagre-EPF. Of note, we did not observe tarsal plate reactivity in sporadic PF sera that did recognize meibomian glands. In addition, some preliminary experiments showed different patterns of autoreactivity to human heart muscle and leg skeletal muscle microarray slides (Imgenex) that did not seem to colocalize with connexin-43, a gap junction protein. In this regard, we need to perform more extensive experiments. We conclude that, in our experiments, the partial prefixation of the skin substrate with paraformaldehyde greatly assisted the process of unmasking target antigens within the meibomian glands and the tarsal muscle. The identity of the antigens in this polyclonal immune response remains to be elucidated. The autoimmune bullous skin diseases, pemphigus (with major subsets pemphigus vulgaris, PF, and paraneoplastic pemphigus) and the more common bullous pemphigoid (with variant disease phenotypes of cicatricial pemphigoid and gestational pemphigoid) may have ocular manifestations. As such, a comparison of all of these bullous diseases needs to be performed.

We thank Drs Hector Dario Escobar and Liliana Zuluaga, ophthalmologists, from the Institute of Health Science (Instituto de Ciencias de la Salud), Medellin, Colombia, South America, for their clinical evaluation of patients. We also want to thank Dr Weiqing Gao at the Montgomery Eye Pathology Laboratory of the Department of Ophthalmology at Emory University Medical Center for her excellent technical assistance.

REFERENCES

1. Viera J. Pemphigus foliaceus (fogo selvagem): endemic disease of Sao Paolo (Brazil). Arch Dermatol Syph 1940; 211:858.
2. Proenca N, Ribeira A. Aspectus epidemiologicos do penfigo foliaceo no Brazil [Epidemiologic features of pemphigus foliaceus in Brazil]. Rev Assoc Med Bras 1976;22:281-4.
3. Castro R, Proenca N. Semelhancas e diferencas entre o fogo selvagem e o penfigo foliaceo de Cazenave [Similarities and differences between South American pemphigus foliaceus and Cazanave's pemphigus foliaceus]. An Bras Dermatol 1983; 53:137-9.
4. Diaz L, Sampaio S, Rivitti EA, Martins CR, Cunha PR, Lombardi C, et al. Endemic pemphigus foliaceus (fogo selvagem): clinical features and immunopathology. J Am Acad Dermatol 1989;20: 657-9.
5. Abréu-Vélez AM, Beutner EH, Montoya F, Bollag WB, Hashimoto T. Analyses of autoantigens in a new form of endemic pemphigus foliaceus in Colombia. J Am Acad Dermatol 2003; 49:609-14.
6. Abréu-Vélez AM, Hashimoto T, Bollag WB, Tobón-Arroyave S, Abreu-Velez CE, Londoño ML, et al. A unique form of endemic pemphigus in Northern Colombia. J Am Acad Dermatol 2003;4 599-80.
7. Evangelista F, Dasher DA, Diaz LA, Prisayanh PS, Li N. E-cadherin is an additional immunological target for pemphigus autoantibodies. J Invest Dermatol 2008;128:1710-8.
8. Lund C, Browder N. The estimate of area of burns. Surg Gynecol Obstet 1944;79:352-8.
9. Labib RS, Rock B, Martins CR, Diaz LA. Pemphigus foliaceus antigen: characterization of an immunoreactive tryptic fragment from BALB/c mouse epidermis recognized by all patients' sera and major autoantibody subclasses. Clin Immunol Immunopathol 1990;57:317-29.
10. Lynch RD, Francis SA, McCarthy KM, Casas E, Thiele C, Schneeberger EE. Cholesterol depletion alters detergent-specific solubility profiles of selected tight junction proteins and the phosphorylation of occluding. Exp Cell Res 2007;313:2597-610.
11. Ameondola F. Ocular manifestations of pemphigus foliaceus. Am J Opthalmol 1949;32:35-44.
12. Steffen C, Thomas D. The men behind the eponym: Francis E. Senear, Barney Usher, and the Senear-Usher syndrome. Am J Dermatopathol 2003;5:432-6.
13. Castro RM, Augusto DAF, Rivitti EA. Sindrome de Senear-Usher e Fogo selvagem (penfigo foliaceo endemico). An Bras Dermatol 1988;63(Suppl):264-5.
14. Serri F, Huber WM. The development of sebaceous glands in man. In: Montagna W, Ellis RA, Silvers AF, editors. Advances in biology of skin. Vol 4. The sebaceous glands. New York: Pergamon Press; 1963. p. 1.
15. Den S, Shimizu K, Ikeda T, Tsubota K, Shimmura S, Shimazaki J. Association between meibomian gland changes and aging, sex, or tear function. Cornea 2006;25:651-5.
16. Tsai PS, Evans JE, Green KM, Sullivan RM, Schaumberg DA, Richards SM, et al. Proteomic analysis of human meibomian gland secretions. Br J Ophthalmol 2006;90:372-7.
17. Castro RM, Proença NG. Similarities and differences between Brazilian wild fire and pemphigus foliaceus Cazenave. Hautarzt 1982;11:574-7.
18. Stanley JR, Koulu L, Thivolet C. Distinction between epidermal antigens binding pemphigus vulgaris and pemphigus foliaceus autoantibodies. J Clin Invest 1984;74: 313-20.

19. Shirakata Y, Amagai M, Hanakawa Y, et al. Lack of mucosal involvement in pemphigus foliaceus may be due to low expression of desmoglein 1. J Invest Dermatol 1998;110: 76-8.
20. Montagna W, Parakkal PF. The structure and function of skin. 3rd ed. New York: Academic Press; 1974.
21. Gupta N, DeFranco AL. Visualizing lipid raft dynamics and early signaling events during antigen receptor-mediated B-lymphocyte activation. Mol Biol Cell 2003;14:432-44.
22. Brown DA, London E. Functions of lipid rafts in biological membranes. Annu Rev Cell Dev Biol 1998;14:111-36.
23. Metze D, Jurecka W, Gebhart W, Schmidt J, Mainitz M, Niebauer G. Immunohistochemical demonstration of immunoglobulin A in human sebaceous and sweat glands. J Invest Dermatol 1989;1:13-7.
24. Simons K, Toomre D. Lipid rafts and signal transduction. Nat Rev Mol Cell Biol 2000;1:31-9.
25. Daoud YJ, Foster CS, Ahmed R. Eyelid skin involvement in pemphigus foliaceus. Ocul Immunol Inflamm 2005;13: 389-94.
26. Palleschi GM, Giomi B, Fabbri P. Ocular involvement in pemphigus. Am J Ophthalmol 2007;144:149-52.

Paraneoplastic Pemphigus Associated with Malignant Gastrointestinal Stromal Tumour

Takashi Masu[1,2], Ryuhei Okuyama[1]*, Takahiko Tsunoda[2], Takashi Hashimoto[3] and Setsuya Aiba[1]

Department of Dermatology, [1]Tohoku University Graduate School of Medicine, 1-1 Seiryo-machi, Aoba-ku, 980-8574, Sendai and [3]Kurume University Graduate School of Medicine, Kurume and [2]Division of Dermatology, Yamagata City Hospital Saiseikan, Yamagata, Japan. E-mail: rokuyama@mail.tains.tohoku.ac.jp

Accepted July 1, 2009.

Sir,

Paraneoplastic pemphigus (PNP) is an autoimmune bullous disease characterized by severe mucous membrane involvement, polymorphous skin eruptions, and underlying neoplasms. Most cases are associated with lymphoproliferative neoplasms, and solid tumours have rarely been associated with PNP (1, 2). We describe here a patient with PNP associated with malignant gastrointestinal stromal tumour (GIST).

CASE REPORT

A 57-year-old woman had a 1-month history of painful erosions in the oral cavity and skin eruptions on her trunk and extremities. Physical examination revealed multiple well-demarcated erosions on the lower lip and oral mucosa, together with fine oedematous erythema on her back and extremities (Fig. 1a). Standard laboratory tests yielded normal findings, except for a slightly increased C-reactive protein level (0.68 mg/dl). The biopsy specimens taken from the erythema on the dorsum of the foot showed vacuolar interface dermatitis with scattered individual keratinocyte necrosis and perivascular lymphohistiocytic infiltration in the papillary dermis.

Her skin lesions worsened significantly during the following 6 weeks. She developed severe stomatitis, pseudomembranous conjunctivitis, and blisters on her extremities associated with fever and general fatigue (Fig. 1b). The second biopsy specimen obtained from a bullous lesion on her forearm revealed suprabasal cleft with acantholysis. Indirect immunofluorescence on normal human skin revealed cell surface staining, up to a titre of 1: 160 (Fig. 1c). Enzyme-linked immunosorbent assay revealed increased antibodies against desmoglein 3 (40.03; normal < 7.0), desmoglein 1 (15.96; < 14.0) and bullous pemphigoid antigen 180 (104.50; < 9.0). Immunoblot analysis using an ethylenediaminetetraacetic acid (EDTA)-separated human skin extract was performed as described previously (3) and revealed the presence of autoantibodies reactive with a doublet of PNP antigen, the 210-kDa envoplakin and 190-kDa periplakin (Fig. 2). In addition, the 130-kDa desmoglein 3 antibody also developed with the exacerbation. According to the clinical, histological, and immunopathological findings, a diagnosis of PNP was made.

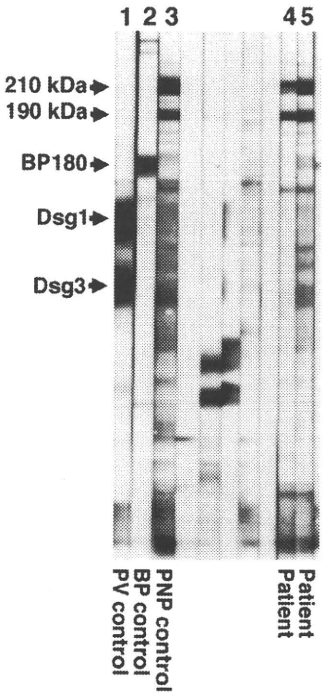

Fig. 2. Results of immunoblot analysis. Patient sera taken on two different occasions (*lane 4 and 5*) recognized 210-kDa envoplakin and 190-kDa periplakin, which were also detected by control paraneoplastic pemphigus (PNP) serum (*lane 3*). Lanes 1–3 show the reactivity of the control sera. Pemphigus vulgaris serum reacted with 160-kDa desmoglein (Dsg) 1 and 130-kDa Dsg 3 (*lane 1*), and bullous pemphigoid (BP) serum with 180-kDa BP antigen (*lane 2*).

In a malignancy survey, whole body computed tomography revealed a 7-cm mass within the abdominal cavity (Fig. 3a). Surgical resection was performed. A multi-nodular tumour, 10 × 7-cm in size, was located within the omentum and was removed en bloc. The tumour consisted of a uniform population of spindle cells with occasional mitoses (Fig. 3b). The spindle cells were arranged in short fasicles with nuclear palisading. The tumour was diagnosed as malignant GIST because the spindle cells stained positively for CD117 antigen. After the operation, the patient was treated with prednisolone at a dose of 60 mg per day. The mucosal lesions healed slowly with a remarkable improvement in the cutaneous lesions. The dose of prednisolone was slowly tapered. However, 4 months after the operation she died after the sudden development of dyspnoea.

Fig. 1. Clinical and histopathological views. (a) Well-demarcated erosions on the lower lip and tongue. (b) Bullae on the oedematous erythema of the arm. (c) Indirect immunofluorescence of patient serum on human skin demonstrating binding of IgG to the cell surface.

DISCUSSION

In the majority of patients with PNP, the clinical course is progressive and often fatal, even if the underlying malignancies are removed completely. Respiratory failure, in particular, is a common terminal event. Approximately 30–40% of cases develop pulmonary injury by acantholysis of the bronchial epithelium (4). For diagnosis of PNP, detection of autoantibodies by immunoprecipitation is important. Compared with the immunoprecipitation, immunoblotting is easier and less hazardous. Although the immunoblotting detects 250-kDa/210-kDa desmoplakin I/II and 230-kDa bullous pemphigoid antigen less frequently, all the PNP sera exhibit characteristic reactivity with 210-kDa envoplakin and 190-kDa periplakin in immunoblotting with a human epidermal extract (3).

The majority of malignancies associated with PNP are lymphoproliferative disorders, including non-Hodgkin's B-cell lymphoma, chronic lymphocytic leukaemia, Castleman's disease and thymoma (1, 2). Other malignancies can also be associated with PNP, including soft tissue sarcomas (5–7), and even pancreas, uterine and hepatocellular carcinomas (8–10). To our knowledge, PNP has not yet been described in association with GIST. GIST is a rare primary neoplasm of the gastrointestinal tract, mesentery, or omentum. Although the exact pathogenesis is not fully known, it is thought to originate from the same lineage as the interstitial cells of Cajal, pacemaker cells of the gastrointestinal tract. In many, but not all cases of GIST, mutations occur in KIT proto-oncogene, a tyrosine kinase receptor, which leads to ligand independent activation (11). The tumour size and mitotic count are prognostic factors. The present case was considered to involve an aggressive tumour because it was larger than 5 cm with more than five mitoses per 50 high-powered field (12, 13). This case suggests that GIST can be added to the list of associated tumours in PNP.

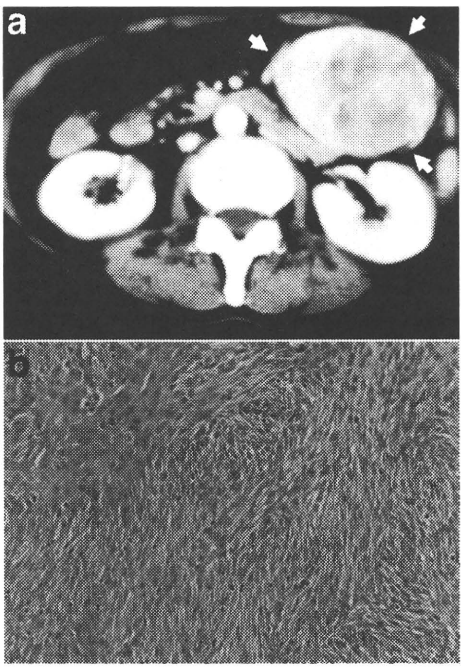

Fig. 3. Abdominal gastrointestinal stromal tumour. (a) Abdominal computed tomography showing the tumour mass (*arrows*). (b) Surgical resection biopsy. Spindle-shaped cells are arranged in cords and were associated with atypical mitoses (haematoxylin and eosin (H&E) ×200).

REFERENCES

1. Anhalt GJ, Kim SC, Stanley JR, Korman NJ, Jabs DA, Kory M, et al. Paraneoplastic pemphigus. An autoimmune mucocutaneous disease associated with neoplasia. N Engl J Med 1990; 323: 1729–1735.
2. Horn TD, Anhalt GJ. Histologic features of paraneoplastic pemphigus. Arch Dermatol 1992; 128: 1091–1095.
3. Hashimoto T, Amagai M, Watanabe K, Chorzelski TP, Bhogal BS, Black MM, et al. Characterization of paraneoplastic pemphigus autoantigens by immunoblot analysis. J Invest Dermatol 1995; 104: 829–834.
4. Fullerton SH, Woodley DT, Smoller BR, Anhalt GJ. Paraneoplastic pemphigus with autoantibody deposition in bronchial epithelium after autologous bone marrow transplantation. JAMA 1992; 267: 1500–1502.
5. Kaplan I, Hodak E, Ackerman L, Mimouni D, Anhalt GJ, Calderon S. Neoplasms associated with paraneoplastic pemphigus: a review with emphasis on non-hematologic malignancy and oral mucosal manifestations. Oral Oncol 2004; 40: 553–562.
6. Wang J, Bu DF, Li T, Zheng R, Zhang BX, Chen XX, et al. Autoantibody production from a thymoma and a follicular dendritic cell sarcoma associated with paraneoplastic pemphigus. Br J Dermatol 2005; 153: 558–564.
7. Kahawita IP, Fernando MS, Sirimanna GM, Fernando R, de Silva MV. Paraneoplastic pemphigus associated with inflammatory myofibroblastic tumor. Int J Dermatol 2006; 45: 1394–1396.
8. Hinterhuber G, Drach J, Riedl E, Bohler K, Ferenci P, Wolff K, et al. Paraneoplastic pemphigus in association with hepatocellular carcinoma. J Am Acad Dermatol 2003; 49: 538–540.
9. Matz H, Milner Y, Frusic-Zlotkin M, Brenner S. Paraneoplastic pemphigus associated with pancreatic carcinoma. Acta Derm Venereol 1997; 77: 289–291.
10. Niimi Y, Kawana S, Hashimoto T, Kusunoki T. Paraneoplastic pemphigus associated with uterine carcinoma. J Am Acad Dermatol 2003; 48: S69–S72.
11. Hirota S, Isozaki K, Moriyama Y, Hashimoto K, Nishida T, Ishiguro S, et al. Gain-of-function mutations of c-kit in human gastrointestinal stromal tumors. Science 1998; 279: 577–580.
12. Miettinen M, Sobin LH, Lasota J. Gastrointestinal stromal tumors of the stomach: a clinicopathologic, immunohistochemical, and molecular genetic study of 1765 cases with long-term follow-up. Am J Surg Pathol 2005; 29: 52–68.
13. Kroep JR, Bovée JVMG, van der Molen AJ, Hogendoorn PCW, Gelderblom H. Extra-abdominal subcutaneous metastasis of a gastrointestinal stromal tumor: report of a case and a review of the literature. J Cutan Pathol 2009; 36: 565–569.

A Homozygous Nonsense Mutation within the Dystonin Gene Coding for the Coiled-Coil Domain of the Epithelial Isoform of BPAG1 Underlies a New Subtype of Autosomal Recessive Epidermolysis Bullosa Simplex

Richard W. Groves[1,2], Lu Liu[3], Patricia J. Dopping-Hepenstal[3], Hugh S. Markus[4], Patricia A. Lovell[3], Linda Ozoemena[3], Joey E. Lai-Cheong[1,2], Jeffrey Gawler[5], Katsushi Owaribe[6], Takashi Hashimoto[7], Jemima E. Mellerio[1,2], John B. Mee[2] and John A. McGrath[2]

Epidermolysis bullosa (EB) is a group of autosomal dominant and recessive blistering skin diseases in which pathogenic mutations have been reported in 13 different genes encoding structural proteins involved in keratinocyte integrity, as well as cell–matrix or cell–cell adhesion. We now report an inherited skin fragility disorder with a homozygous nonsense mutation in the dystonin gene (*DST*) that encodes the coiled-coil domain of the epithelial isoform of bullous pemphigoid antigen 1, BPAG1-e (also known as BP230). The mutation, p.Gln1124X, leads to the loss of hemidesmosomal inner plaques and a complete absence of skin immunostaining for BPAG1-e, as well as reduced labeling for plectin, the β4 integrin subunit, and for type XVII collagen. The 38-year-old affected individual has lifelong generalized trauma-induced spontaneous blisters and erosions, particularly around the ankles. In addition, he experiences episodic numbness in his limbs, which started at the age of 37 years. These neurological symptoms may also be due to *DST* gene mutation, although he has a concomitant diagnosis of CADASIL (cerebral arteriopathy, autosomal dominant, with subcortical infarcts and leukoencephalopathy), a cerebral small-vessel arteriopathy, which thus complicates the genotype–phenotype interpretation. With regard to skin blistering, the clinicopathological findings expand the molecular basis of EB by identifying BPAG1-e pathology in a new form of autosomal recessive EB simplex.

Journal of Investigative Dermatology (2010) **130,** 1551–1557; doi:10.1038/jid.2010.19; published online 18 February 2010

INTRODUCTION

The group of inherited blistering skin diseases, known as epidermolysis bullosa (EB), represents a diverse collection of autosomal dominant and autosomal recessive disorders with varying skin, mucous membrane, and extracutaneous abnormalities (Fine *et al.*, 2008; Fine and Mellerio, 2009a, b). Originally classified into three main subtypes, namely EB simplex, junctional EB, and dystrophic EB, on the basis of the level of tissue cleavage at or close to the dermal–epidermal junction (DEJ), the latest classification of EB has been expanded to include other cell–cell or cell–matrix adhesion disorders (Fine *et al.*, 2008). Thus, the term "EB" now encompasses inherited disorders of hemidesmosome attachment complexes, keratin intermediate filaments, focal adhesions, and desmosome cell junctions, and involves pathogenic mutations in 13 genes encoding 11 different structural proteins (Fine *et al.*, 2008).

One skin protein that has not yet been implicated in the pathogenesis of EB, however, is bullous pemphigoid antigen 1 (BPAG1-e) (also known as BP230), a key component of hemidesmosomes and a member of the plakin family with cytoskeletal linker properties (Borradori and Sonnenberg, 1999; Leung *et al.*, 2001a; Litjens *et al.*, 2006; Sonnenberg and Liem, 2007). BPAG1-e is encoded for by the dystonin (*DST*) gene, the alternative splicing of which may give rise to

[1]*St John's Institute of Dermatology, The Guy's and St Thomas' NHS Foundation Trust, St Thomas' Hospital, London, UK;* [2]*Division of Genetics and Molecular Medicine, King's College London, Guy's Hospital, London, UK;* [3]*The Robin Eady National Diagnostic Epidermolysis Bullosa Laboratory, GSTS Pathology, St Thomas' Hospital, London, UK;* [4]*Department of Clinical Neuroscience, St George's University of London, London, UK;* [5]*145 Harley Street, London, UK;* [6]*Division of Biological Science, Graduate School of Science, Nagoya University, Nagoya, Japan and* [7]*Department of Dermatology, Kurume University School of Medicine, Kurume, Fukuoka, Japan*

Correspondence: John A. McGrath, Dermatology Research Laboratories, 9th Floor, Tower Wing, Guy's Hospital, Great Maze Pond, London SE1 9RT, UK. E-mail: john.mcgrath@kcl.ac.uk

Abbreviations: BPAG1, bullous pemphigoid antigen 1; CADASIL, cerebral arteriopathy, autosomal dominant, with subcortical infarcts and leukoencephalopathy; DEJ, dermal-epidermal junction; DST, dystonin; EB, epidermolysis bullosa

Received 31 October 2009; revised 13 December 2009; accepted 3 January 2010; published online 18 February 2010

multiple tissue isoforms with variable expression in the skin, neurons, muscles, and the central nervous system (Leung *et al.*, 2001b; Jefferson *et al.*, 2006; Young and Kothary, 2007, 2009). The main isoform expressed in the central nervous system is BPAG1-a, although a further neural variant, BPAG1-n, may also exist; whether BPAG1-n is expressed *in vivo*, however, is uncertain (Leung *et al.*, 2001b). In muscle, the main isoform is BPAG1-b. In the skin, there is a predominance of BPAG1-e, but some BPAG1-a (and perhaps BPAG1-n) may also be present (Sonnenberg and Liem, 2007). Details of these *DST* splice variants and their functional subdomains are illustrated in Supplementary Figure S1 online.

Mutations in the mouse *Dst* gene have previously been shown to cause sensory neuron degeneration and skin fragility (Brown *et al.*, 1995; Guo *et al.*, 1995; Pool *et al.*, 2005; Goryunov *et al.*, 2007), but no human *DST* gene pathology has been reported, apart from a t(6;15)(p11.2;p12) translocation in a 4-year-old girl that resulted in encephalopathy, severe motor and mental retardation, and delayed visual maturation (Giorda *et al.*, 2004). In that case, the chromosome 6 break point was between the BPAG1-a and BPAG1-b isoforms, but no abnormality of BPAG1-e was evident.

We now report details of an individual with a naturally occurring homozygous nonsense mutation in part of the *DST* gene that encodes for the coiled-coil domain, which is exclusively expressed in BPAG1-e and BPAG1-n isoforms.

RESULTS

Clinical features of skin blistering and neurological symptoms

The affected individual was a 38-year-old Kuwaiti man born to distantly related parents. He was the second of five siblings and the only one with a history of blisters. His two children had no skin symptoms and there was no family history of skin fragility or blistering. The patient had experienced lifelong trauma-induced spontaneous blisters and erosions, particularly around his ankles and feet (Figure 1a), although the face, trunk, and more proximal limbs were also affected. Blisters and erosions healed without delay, scarring, or milia formation. Blistering was associated with skin peeling and occasional hemorrhage, as well as hypopigmentation and some postinflammatory hyperpigmentation. Nail dystrophy of all toenails was present, particularly affecting the great toes. Hair growth was normal. There was no history of mucosal blistering, although moderate dental caries and reactive gingival inflammation were evident. The patient reported no gastrointestinal or urological symptoms.

In addition to skin blistering, the patient had a few years' history of neurological symptoms, including two episodes of collapse, recurrent bilateral headaches, and transient episodes of left arm numbness and weakness lasting a few

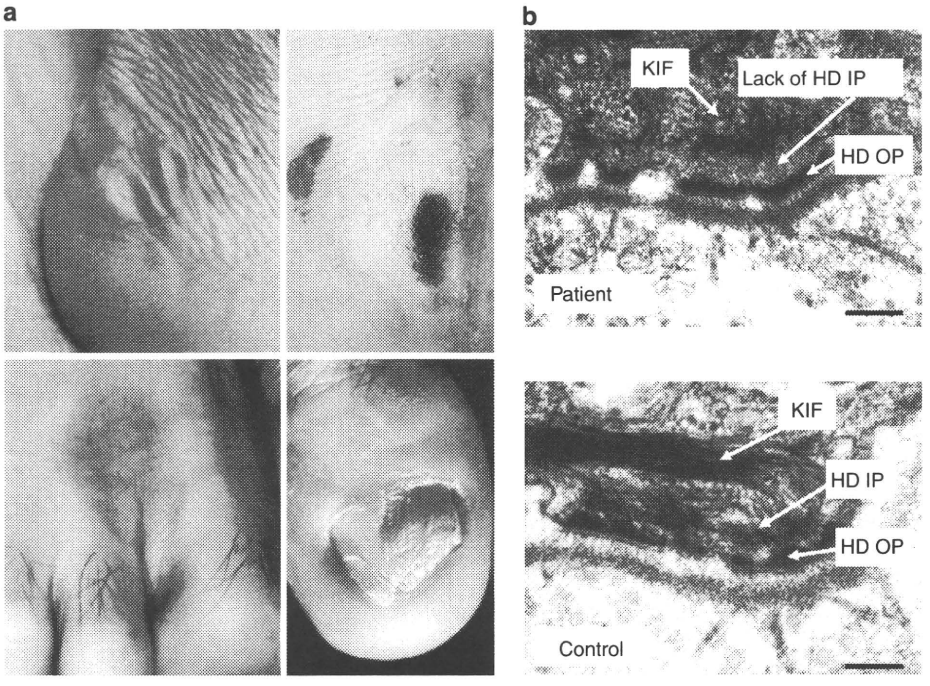

Figure 1. Ultrastructural abnormalities of hemidesmosomal inner plaques provide clues to the pathology of a new inherited skin fragility disorder. (**a**) Clinically, there is a blister measuring 2.5 × 1.5 cm on the right heel, as well as an area of earlier blistering on the right sole showing reepithelialization, some scale, minor hemorrhage, but no scarring. Other features include postinflammatory hyperpigmentation on the dorsal aspect of the right foot close to the great and second toes at the site of the old blistering, and dystrophy of the right great toe nail after previous trauma (no fungus was present on microscopy and culture). (**b**) Transmission electron microscopy of the dermal–epidermal junction (DEJ) in patient skin shows keratin intermediate filaments (KIFs) and hemidesmosomal outer plaques (HD OP), but a lack of hemidesmosomal inner plaques (HD IP). In contrast, transmission electron microscopy of the DEJ in normal control skin reveals that HDs have clearly defined HD IPs and HD OPs (bar = 100 nm).

seconds at a time. There was no history of stroke or depression. Both parents were deceased; his mother died at the age of 56 years after multiple strokes. He had two sisters and three brothers, one of whom had been given a diagnosis of "multiple sclerosis" after a number of neurological events that were consistent with minor strokes. Magnetic resonance brain imaging in our patient showed scattered white matter hyperintensities, but no involvement of the anterior temporal pole and the external capsule. Normal investigations included the following: intracranial and extracranial magnetic resonance angiography, cerebrospinal fluid examination including oligoclonal bands, visual brainstem, and somatosensory evoked potentials. On the basis of family history, abnormal magnetic resonance imaging, and neurological symptoms, he had a concomitant diagnosis of autosomal dominant cerebral small-vessel arteriopathy CADASIL (cerebral arteriopathy, autosomal dominant, with subcortical infarcts and leukoencephalopathy; MIM125310) (Joutel *et al.*, 1996).

Thus, our patient had a history of skin blistering resembling a form of EB; his mother, brother, and he had neurological histories consistent with CADASIL.

Transmission electron microscopy of the DEJ reveals abnormal hemidesmosomal inner plaques

The primary clue to the molecular pathology responsible for skin fragility came from ultrastructural observations and a candidate gene approach. Although no blisters or microsplits were noted at or close to the DEJ, discrete abnormalities of hemidesmosomes were evident. There were no differences from control skin in the overall number of hemidesmosomes, but the morphology of individual hemidesmosomes was abnormal. Notably, the inner plaques were poorly formed or completely absent, leading to a lucent zone between keratin filaments and the outer hemidesmosomal plaques (Figure 1b). The keratin filaments extended to where the inner plaques should be, but did not seem to associate with any plasma membrane attachment structure. The outer hemidesmosomal plaques, however, showed no gross abnormalities. Similarly, sub-basal dense plates, anchoring filaments, the lamina lucida, the lamina densa, and anchoring fibrils, were all within normal limits. Thus, transmission electron microscopy provided the specific ultrastructural clue that an abnormality of a gene encoding a structural component of the hemidesmosomal inner plaque might underlie the skin fragility in this patient. We also searched for granular osmiophilic material around vascular smooth muscle in the deep dermis, as this has been noted as a specific ultrastructural feature of CADASIL (Ishiko *et al.*, 2005), but did not identify pathognomonic changes.

Immunofluorescence microscopy and immunoblotting show an absence of BPAG1-e expression in skin/keratinocytes

Immunolabeling of the DEJ in the patient's skin showed reduced-intensity staining for several hemidesmosome-associated proteins. Notably, there was a complete absence of immunoreactvity using a BPAG1-e-specific antibody (BPC319, directed against the carboxyl terminal domain of BPAG1-e, Okumura *et al.*, 2002) compared with bright, linear labeling at the DEJ in control skin (Figure 2a). Immunoblotting using keratinocyte extracts and an additional BPAG1-e antibody (5E, directed against the carboxyl terminal domain of BPAG1-e, Hashimoto *et al.*, 1993) showed a complete absence of BPAG1-e in the patient's cells (Figure 2b). Immunostaining of skin sections from the patient also revealed markedly reduced labeling for the β4 integrin subunit at the DEJ, moderately reduced plectin immunoreactivity, and slightly diminished type XVII collagen immunolabeling (Supplementary Figure S2 online). No differences compared with control skin were noted for the α6 integrin subunit, as well as for keratin 14, laminin-332, collagen IV, or collagen VII (Supplementary Figure S2 online).

***DST* mutation screening identifies a homozygous nonsense mutation in the coiled-coil domain, present in BPAG1-e and BPAG1-n isoforms**

Sequencing of the patient's genomic DNA identified a homozygous C>T transition (c.3478C>T; GenBank NM_001723.4) that converts glutamine to a stop codon, designated p.Gln1124X (Figure 2c). This mutation occurs within the coiled-coil domain, a region that is not present in BPAG1-a or BPAG1-b (Supplementary Figure S1 online). This mutation was not identified in screening 200 ethnically matched control chromosomes. Sequencing of the *PLEC1* gene encoding plectin and the *ITGB4* gene encoding the β4 integrin subunit was also performed, but no pathogenic mutations were identified.

The nonsense mutation in *DST* does not lead to a major reduction in mRNA levels relevant to the BPAG1-e isoform

The mutation, p.Gln1124X, occurs in the penultimate exon of the transcript encoding BPAG1-e (exon 23 of 24). We assessed the consequences of the mutation in gene expression by performing real-time reverse transcriptase-PCR using RNA extracted from the patient and control skin and creating different primer pairs upstream of the mutation, spanning the mutation in the coiled-coil domain, and in the 3′ untranslated region (Figure 2d). Gene expression levels in the patient were reduced by ~25% in the 3′ untranslated region. In contrast, there was only a very slight reduction (<3%) for the other primer pairs.

***NOTCH3* mutation screening identifies a heterozygous cysteine substitution consistent with a concomitant diagnosis of CADASIL**

Sequencing of the patient's genomic DNA identified a heterozygous G>C transversion (c.1790G>C; GenBank U97669) in exon 11 of *NOTCH3* that converts cysteine to serine, designated p.Cys597Ser (not illustrated). This mutation is typical of CADASIL, in which mutations result in unpairing of a cysteine–cysteine bond in one of the epidermal growth factor-like repeats present in the extracellular portion of the transmembranous NOTCH3 protein (Joutel *et al.*, 1997). This mutation was not detected in screening 200 ethnically matched control chromosomes.

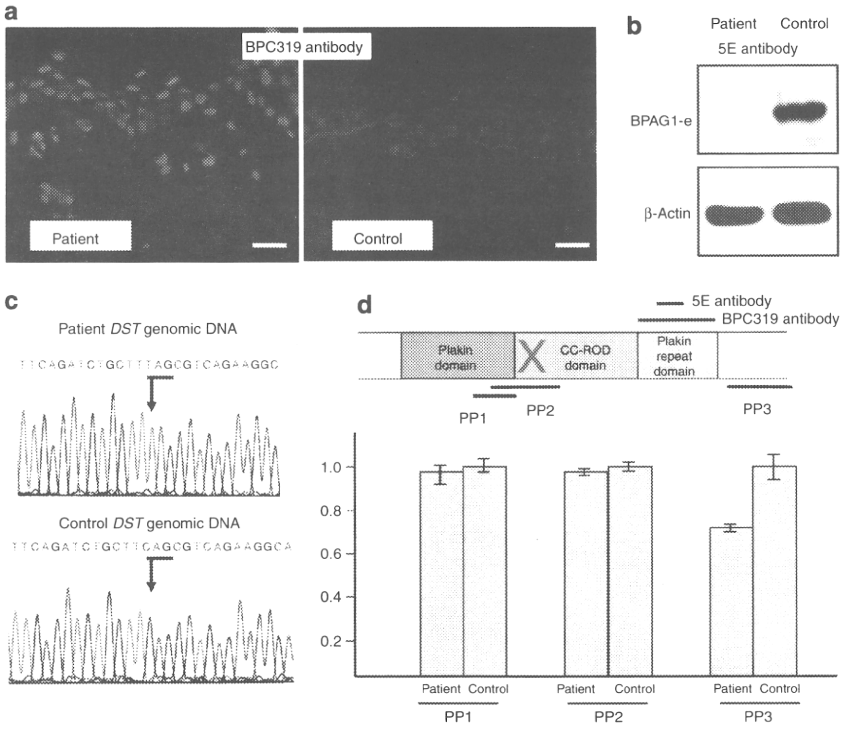

Figure 2. Loss of BPAG1-e protein expression due to a homozygous nonsense mutation in the *DST* gene. (**a**) Immunofluorescence microscopy using an antibody that recognizes the carboxyl terminal region of bullous pemphigoid antigen 1 (BPAG1)-e (clone BPC319) reveals completely undetectable immunostaining in patient skin in contrast to linear labeling at the dermal-epidermal junction (DEJ) in normal control skin. (Bar = 50 μm). (**b**) Immunoblotting using extracts from cultured keratinocytes shows a complete absence of BPAG1-e in patient material compared with control (clone 5E, carboxyl terminal region of BPAG1-e). (**c**) DNA sequencing reveals a homozygous nonsense mutation partly of the *DST* gene coding for the coiled-coil domain of BPAG1-e (and BPAG1-n). In patient genomic DNA, there is a homozygous C > T transition (c.3478C > T, GenBank NM_001723.4) that converts glutamine to a stop codon (p.Gln1124X) that is not present in wild-type sequencing. (**d**) Real-time reverse transcriptase (RT)-PCR using primer sets upstream from the mutation (PP1) and spanning the mutation in the coiled-coil domain (PP2) shows that the nonsense mutation does not lead to mRNA decay. For the primer sited in the 3′ untranslated region (UTR) (PP3), patient mRNA is reduced by only ~25%, consistent with a nonsense mutation in the penultimate exon of a gene transcript not triggering substantial mRNA decay. The schematic illustrates how RT-PCR primers relate to the domains of BPAG1-e. This schematic also illustrates the epitopes of BPAG1-e corresponding to the antibodies used for the data shown in panels **a** and **b**.

DISCUSSION

DST mutation and inherited skin fragility

Delineation of a homozygous nonsense mutation in *DST* expands the number of basement membrane genes and proteins implicated in the pathogenesis of the different forms of EB, and also highlights the importance of hemidesmosomes in maintaining epidermal integrity (Supplementary Figure S3 online). Hemidesmosomes are intricate multiprotein adhesion complexes that provide a stable attachment between the basement membrane and the stratified (and other) epithelia (Litjens *et al.*, 2006). In the skin, hemidesmosomes are composed of BPAG1-e, plectin, α6β4 integrin, tetraspanin CD151, and type XVII collagen. Together, these proteins form an intricate network that provides a structural bridge extending from keratin intermediate filaments in basal keratinocytes to the collagen fibers within the papillary dermis (Koster *et al.*, 2003). Both BPAG1-e and plectin bind to keratin filaments. For BPAG1-e, the binding to keratin occurs through its carboxyl domain, whereas its amino terminus binds to the cytoplasmic domain of type XVII collagen (Borradori and Sonnenberg, 1999; Hopkinson and Jones, 2000; Fontao *et al.*, 2003), as well as to β4 integrin and erbin (Favre *et al.*, 2001). Plectin also binds to β4 integrin (de Pereda *et al.*, 2009), and β4 integrin binds to erbin (Favre *et al.*, 2001).

The homozygous nonsense mutation in our patient led to a loss of BPAG1-e protein expression at the DEJ and in keratinocytes, as determined by immunofluorescence microscopy and western blotting using two antibodies directed against the carboxyl terminus of BPAG1-e. Nonsense mutations typically lead to mRNA decay, except when located in the last exon or the distal part of the penultimate exon (Mühlemann *et al.*, 2008; Neu-Yilik and Kulozik, 2008; Silva and Romão, 2009). The mutation p.Gln1124X is located within the proximal part of the penultimate exon but does not seem to lead to substantial mRNA decay. Nevertheless, immunostaining of the patient's skin sections showed reduced labeling for several other hemidesmosomal components that directly or indirectly associate with the amino and carboxyl domains of BPAG1-e. It is noteworthy that there was reduced protein labeling for the β4 integrin subunit, as well as for plectin and type XVII collagen. The most marked reduction in labeling was for β4 integrin, which is of interest, given recent data showing

that BPAG1-e maintains keratinocyte polarity through β4 integrin-mediated modulation of Rac1 and cofilin activation (Hamill *et al.*, 2009).

Ultrastructurally, the *DST* mutation was associated with loss of the hemidesmosomal inner plaque, but not with gross changes in the size or number of hemidesmosomal outer plaques, sub-basal dense plates, anchoring filaments, or anchoring fibrils. Keratin filaments were still seen in close apposition to the missing inner plaques, although no clear attachment structures for the filaments were evident. Although none of the skin biopsy samples obtained from the patient provided histological evidence for the level of blister formation, it is highly likely that cleavage occurred through the level of the missing inner hemidesmosomal plaques, and thus the subtype of skin fragility is probably best classified as an autosomal recessive form of EB simplex. Compared with other forms of autosomal recessive EB simplex, the severity of skin blistering in our patient was relatively mild, indicating a comparatively minor role in maintaining hemidesmosomal integrity for BPAG1-e compared with other hemidesmosome-associated proteins.

DST mutation and clinical neuropathology

In our patient, the clinical features also included some neurological abnormalities, including headaches and parasthesiae. A key question is whether these symptoms and signs are due to his *DST* gene pathology or due to a separate disorder. In support of the latter, screening of the *NOTCH3* gene identified a heterozygous missense mutation that was typical of CADASIL, an autosomal dominant small-vessel arteriopathy. In this disorder, vascular changes can be seen in the small arteries throughout the body, but clinical features are limited to the central nervous system. These include early-onset lacunar stroke, migraine usually with aura, depression, and early-onset vascular dementia. Our patient was reviewed in a UK National CADASIL clinic, however, and it was believed that these neurological symptoms were not typical of CADASIL symptomotology, suggesting perhaps that *DST* gene pathology might also be a contributing factor.

There are a number of publications linking abnormalities in the *DST* gene and BPAG1-e protein to human neurological abnormalities. Notably, there is an epidemiological association between patients with the subepidermal blistering disease, bullous pemphigoid, and an increased incidence of multiple sclerosis and also Parkinson's disease (Stinco *et al.*, 2005), as well as epilepsy, dementia, and stroke (Foureur *et al.*, 2001, 2006). Moreover, autoantibodies to BPAG1-e have been associated with various neurological disorders (Li *et al.*, 2009), and have been identified in the cerebrospinal fluid of some individuals with multiple sclerosis (Lafitte *et al.*, 2005). The *DST* mutation in our patient is also expected to disrupt BPAG1-n, although the potential significance of this is unknown, given that other studies have failed to demonstrate significant tissue expression of this isoform (Leung *et al.*, 2001b).

Whether our patient's neurological features are the consequence of either *DST* or *NOTCH3* gene pathology or from another cause is still uncertain. To the best of our knowledge, pathogenic mutations in *DST* have not been reported previously, and therefore the future identification of other individuals with additional mutations in this gene will be necessary to clarify genotype–phenotype correlation. For now, delineation of a homozygous loss-of-function mutation in the *DST* gene expands the molecular basis of inherited skin blistering and demonstrates the particular *in vivo* role of BPAG1-e in the structural organization of hemidesmosomes at the cutaneous basement membrane zone.

MATERIALS AND METHODS

Patient and biological samples

The patient provided written and informed consent according to a protocol approved by the St Thomas' Hospital Ethics Committee (molecular basis of inherited skin disease: 07/H0802/104). Blood and skin samples (ellipse of skin taken under local anesthesia using 1% lignocaine) were obtained in adherence to the Helsinki guidelines. The skin sampled was noninflamed, nonlesional skin, as, at the time of examination, the patient had no fresh blisters (i.e., <24 hours old).

Transmission electron microscopy

Skin biopsy specimens were cut into small pieces (of $<1\,mm^3$) and fixed in half-strength Karnovsky fixative for 4 hours at room temperature. After washing in 0.1 M phosphate buffer (pH 7.4), the samples were immersed in 1.3% aqueous osmium tetroxide (TAAB Laboratories, Berkshire, UK) for 2 hours, followed by incubation in 2% uranyl acetate (Bio-Rad, Hertfordshire, UK), and dehydrated in a graded ethanol series, and then embedded in epoxy resin via propylene oxide (TAAB Laboratories). Ultra-thin sections were stained with uranyl acetate and lead citrate and examined in a Philips CM10 transmission electron microscope (Philips, Eindhoven, The Netherlands).

Immunofluorescence microscopy

Skin sections measuring 5 μm were air-dried and initially blocked with diluted normal goat serum (Sigma-Aldrich, Dorset, UK), and then incubated with the following antibodies diluted in phosphate-buffered saline with 30% w/v bovine serum albumin (Sigma-Aldrich) where stated: clone BPC319 (BPAG1-e, derived from mice immunized with a recombinant human 361 amino-acid peptide within the carboxyl domain; Okumura *et al.*, 2002), used neat (source K. Owaribe); clone HD1-121 (plectin), 1:40 dilution (K. Owaribe); clones 450-9D (β4 integrin subunit) and GoH3 (α6 integrin subunit), both 1:250 dilutions (AbD Serotec, Oxford, UK); clone mAb-123 (collagen XVII), 1:50 dilution (a gift from M.P. Marinkovich, Stanford, Palo Alto, CA, USA); clone LL002 (keratin 14), 1:1,000 dilution (AbD Serotec); GB3 (laminin-332), 1:300 dilution (http://Immunologicalsdirect.com); clone LH7.2 (collagen VII), 1:1,000 dilution (Sigma-Aldrich, Poole, UK); clone COL94 (collagen IV), 1:500 dilution (Sigma-Aldrich). After washing in phosphate-buffered saline, slides were labeled with fluorescein isothiocyanate secondary antibodies (Invitrogen, Paisley, UK). Negative controls omitting the primary antibody were performed for each set of labeling experiments. All sections were photographed using the same camera and identical exposure times (3 seconds).

DNA sequencing

After obtaining informed consent, genomic DNA was extracted from a peripheral blood sample obtained from the affected

individual. For sequencing, DNA was amplified with primers sited in introns flanking individual exons of the *DST* gene (Supplementary Tables 1 and 2 online) and the *NOTCH3* gene (for further details, see Markus *et al.*, 2002). For PCR amplification, 20 ng genomic DNA was used as a template in an amplification buffer containing 6.25 pmol of primers, 5 mmol of each trinucleotide phosphate, and 0.625 Units Taq polymerase (Qiagen, Warrington, UK) in a total volume of 25 μl in a GeneAmp PCR system 9700 thermal cycler (Applied Biosystems, Crawley, UK). The amplification conditions were 94 °C for 5 minutes, followed by 40 cycles of 94 °C for 30 seconds, 60 °C for 30 seconds, and 72 °C for 45 seconds. Aliquots (5 μl) of PCR products were analyzed by electrophoresis using 3% agarose gel. PCR products were then purified using a QIAquick PCR Purification Kit (Qiagen) and sequenced directly in an ABI 3130 genetic analyzer (Applied Biosystems).

Western blotting

Primary keratinocyte cultures were established as described previously (Mee *et al.*, 2000), and maintained in a defined keratinocyte growth medium (EpiLife, Invitrogen, Renfrew, UK) for three passages. Cellular lysates were prepared from confluent 75 cm^2 flasks through addition of 1 ml preheated lysis buffer (100 mM Tris-Cl (pH 6.8), 4% SDS, 20% glycerol, 0.1% bromophenol blue, 5% β-mercaptoethanol), followed by shearing and clarification. Lysates (12 μl) were separated by denaturing SDS-PAGE using either 5% (BPAG1-e) or 7.5% (β-actin) gels, alongside 5 μl biotinylated markers (Precision Plus Protein WesternC Standards, Bio-Rad, Hemel Hempsted, UK). After transfer to nitrocellulose membranes (Protran BA 85, Whatman, Maidstone, UK), samples were blocked (1 M glycine, 1% ovalbumin, 5% dry skimmed milk, 5% fetal calf serum) for 1 hour at room temperature and probed overnight with either human anti-human BPAG1-e monoclonal antibody (5E, batch 1,748, 1:25 dilution, directed against a 114 amino-acid epitope within the carboxyl domain, source T. Hashimoto) (Hashimoto *et al.*, 1993) or rabbit anti-human β-actin polyclonal antibody (ab8227, Abcam, Cambridge, UK; 1:2,500 dilution) at 4 °C. Detection was accomplished using horseradish peroxidase-conjugated goat anti-rabbit (sc-2054) or goat anti-human (sc-2453) IgG antibody (Santa Cruz Biotechnology, Santa Cruz, CA, USA; 1:3,000 dilution) for 1 hour at room temperature and visualization was achieved using the Amersham ECL Plus Western Blotting Detection System (GE Healthcare, Slough, UK) and autoradiography.

Real-time reverse transcriptase-PCR

Total RNA obtained from patient and normal control skin was extracted using an RNeasy Fibrous Tissue Mini Kit (Qiagen). In all, 0.5 μg of total RNA was used for each 50 μl cDNA synthesis reaction with SuperScript III Reverse Transcriptase (Invitrogen), followed by ribonuclease H (Invitrogen) treatment, according to the manufacturer's protocol. Three sets of PCR primers were generated (PP1, PP2, and PP3, positions illustrated in Figure 2d). PP1 is sited upstream from the mutation (forward primer 5′-AAACGCCGAAGA ATGCAG-3′ nucleotides 3,283–3,300; reverse primer 5′-AATATGC CCCATGTTCAGAAG-3′ nucleotides 3,466–3,446; PCR product size 184 bp; GenBank NM_001724.4). PP2 spans the nonsense mutation (forward primer 5′-TGGACCTAAGGACTCGATATAC-3′ nucleotides 3,332–3,353; reverse primer 5′-TCCTCTACTCGGGACTTTTG-3′ nucleotides 3,584–3,565; PCR product size 253 bp). PP3 is sited in the 3′ untranslated region (forward primer 5′-CTTCAGAACTCCCCT TCATTG-3′ nucleotides 8,371–8,391; reverse primer 5′-GAAATGG GACATTGTGGTAAAC-3′ nucleotides 8,601–8,580; PCR product size 236 bp). The annealing temperature was 55 °C for all reactions. Real-time quantitative PCR was carried out using an ABI Prism 700 Instrument (Applied Biosystems) and SYBR Green PCR Master Mix (Applied Biosystems), following the manufacturer's recommendations. Briefly, 1 μl of cDNA solution was used in 10 μl PCR containing 1 × SYBR Green I master mix with 2.5 mM of $MgCl_2$ and primers. Each sample was run in duplicate, and each PCR run included a no-template control. The 18S ribosomal RNA expression was used as internal reference for relative quantification.

CONFLICT OF INTEREST

The authors state no conflict of interest

ACKNOWLEDGMENTS

Funding for this study was received from the Dystrophic Epidermolysis Bullosa Research Association (DebRA, UK). We also acknowledge financial support from the UK Department of Health through the National Institute for Health Research (NIHR) comprehensive Biomedical Research Centre award to Guy's & St Thomas' NHS Foundation Trust in partnership with King's College London and King's College Hospital NHS Foundation Trust. We are grateful to Masatomo Kawano for help with figure artwork.

SUPPLEMENTARY MATERIAL

Supplementary material is linked to the online version of the paper at http://www.nature.com/jid

REFERENCES

Borradori L, Sonnenberg A (1999) Structure and function of hemidesmosomes: more than simple adhesion complexes. *J Invest Dermatol* 112:411–8

Brown A, Bernier G, Mathieu M *et al.* (1995) The mouse dystonia musculorum gene is a neural form of bullous pemphigoid antigen. *Nat Genet* 10:301–6

de Pereda JM, Lillo MP, Sonnenberg A (2009) Structural basis of the interaction between integrin alpha6beta4 and plectin at the hemidesmosomes. *EMBO J* 28:1180–90

Favre B, Fontao L, Koster J *et al.* (2001) The hemidesmosomal protein bullous pemphigoid antigen 1 and the integrin beta 4 subunit bind to ERBIN. Molecular cloning of multiple alternative splice variants of ERBIN and analysis of their tissue expression. *J Biol Chem* 276:32427–36

Fine JD, Eady RA, Bauer EA *et al.* (2008) The classification of inherited epidermolysis bullosa (EB): Report of the Third International Consensus Meeting on Diagnosis and Classification of EB. *J Am Acad Dermatol* 58:931–50

Fine JD, Mellerio JE (2009a) Extracutaneous manifestations and complications of inherited epidermolysis buillosa: part I. Epithelial associated tissues. *J Am Acad Dermatol* 61:367–84

Fine JD, Mellerio JE (2009b) Extracutaneous manifestations and complications of inherited epidermolysis buillosa: part II. Other organs. *J Am Acad Dermatol* 61:387–402

Fontao L, Favre B, Riou S *et al.* (2003) Interaction of the bullous pemphigoid antigen 1 (BP230) and desmoplakin with intermediate filaments is mediated by distinct sequences within their COOH terminus. *Mol Cell Biol* 14:1978–92

Foureur N, Descamps V, Lebrun-Vignes B *et al.* (2001) Bullous pemphigoid in a leg affected with hemiparesia: a possible relation of neurological diseases with bullous pemphigoid? *Eur J Dermatol* 11:230–3

Foureur N, Mignot S, Senet P *et al.* (2006) Correlation between the presence of type-2 anti-pemphigoid antibodies and dementia in elderly subjects with no clinical signs of bullous pemphigoid. *Ann Dermatol Venereol* 133:439–43

Giorda R, Cerritello A, Bonaglia MA *et al.* (2004) Selective disruption of muscle and brain-specific BPAG1 isoforms in a girl with 6;15 translocation, cognitive and motor delay, and tracheo-oesophageal atresia. *J Med Genet* 41:e71

Goryunov D, Adebola A, Jefferson JJ *et al.* (2007) Molecular characterization of the genetic lesion in Dystonia musculorum (dt-Alb) mice. *Brain Res* 1140:179–87

Guo L, Degenstein L, Dowling J *et al.* (1995) Gene targeting of BPAG1, abnormalities in mechanical strength and cell migration in stratified epithelia and neurologic degeneration. *Cell* 81:233–43

Hamill KJ, Hopkinson SB, Debiase P *et al.* (2009) BPAG1e maintains keratinocyte polarity through β4 integrin-mediated modulation of Rac 1 and cofilin activities. *Mol Biol Cell* 20:2954–62

Hashimoto T, Amagai M, Ebihara T *et al.* (1993) Further analyses of epitopes for human monoclonal anti-basement membrane zone antibodies produced by stable human hybridoma cell lines constructed with Epstein-Barr virus transformants. *J Invest Dermatol* 100:310–5

Hopkinson SB, Jones JC (2000) The N terminus of the transmembrane protein BP180 interacts with the N-terminal domain of BP230, thereby mediating keratin cytoskeleton anchorage to the cell surface at the site of the hemidesmosome. *Mol Biol Cell* 11:277–86

Ishiko A, Shimizu A, Nagata E *et al.* (2005) Cerebral autosomal dominant arteriopathy with subcortical infarcts and leukoencephalopathy (CADASIL): a hereditary cerebrovascular disease, which can be diagnosed by skin biopsy electron microscopy. *Am J Dermatopathol* 27:131–4

Jefferson JJ, Leung CL, Liem RK (2006) Dissecting the sequence specific functions of alternative N-terminal isoforms of mouse bullous pemphigoid antigen 1. *Exp Cell Res* 312:2712–25

Joutel A, Corpechot C, Ducros A *et al.* (1996) Notch3 mutations in CADASIL, a hereditary adult-onset condition causing stroke and dementia. *Nature* 383:707–10

Joutel A, Vahedi K, Corpechot C *et al.* (1997) Strong clustering and stereotyped nature of Notch3 mutations in CADASIL patients. *Lancet* 350:1511–5

Koster J, Geerts D, Favre B *et al.* (2003) Analysis of the interactions between BP180, BP230, plectin and the integrin alpha6beta4 for hemidesmosome assembly. *J Cell Sci* 116:387–99

Lafitte E, Burkhard PR, Fontao L *et al.* (2005) Bullous pemphigoid antigen isoforms: potential new target autoantigens in multiple sclerosis? *Br J Dermatol* 152:537–40

Leung CL, Liem RK, Parry DA *et al.* (2001a) The plakin family. *J Cell Sci* 114:3409–10

Leung CL, Zheng M, Prater SM *et al.* (2001b) The BPAG1 locus: alternative splicing produces multiple isoforms with distinct cytokeletal linker domains, including predominant isoforms in neurons and muscles. *J Cell Biol* 154:691–7

Li L, Chen J, Wang B *et al.* (2009) Sera from patients with bullous pemphigoid (BP) associated with neurological diseases recognized BP antigen 1 in the skin and brain. *Br J Dermatol* 160:1343–5

Litjens SH, de Pereda JM, Sonnenberg A (2006) Current insights into the formation and breakdown of hemidesmosomes. *Trends Cell Biol* 16: 376–83

Markus HS, Martin RJ, Simpson MA *et al.* (2002) Diagnostic strategies in CADASIL. *Neurology* 59:1134–8

Mee JB, Alam Y, Groves RW (2000) Human keratinocytes constitutively produce but do not process interleukin-18. *Br J Dermatol* 143:330–6

Mühlemann O, Eberle AB, Stalder L *et al.* (2008) Recognition and elimination of nonsense mRNA. *Biochim Biophys Acta* 1179:538–49

Neu-Yilik G, Kulozik AE (2008) NMD: multitasking between mRNS surveillance and modulation of gene expression. *Adv Genet* 62:185–243

Okumura M, Yamakawa H, Ohara O *et al.* (2002) Novel alternative splicings of BPAG1 (bullous pemphigoid antigen 1) including the domain structure closely related to MACF (microtubule actin cross-linking factor). *J Biol Chem* 277:6682–7

Pool M, Boudreau Lariviere C, Bernier G *et al.* (2005) Genetic alterations at the Bpag1 locus in dt mice and their impact on transcript expression. *Mamm Genome* 16:909–17

Silva AL, Romão L (2009) The mammalian nonsense-mediated mRNA decay pathway: decay or not to decay! Which players make the decision? *FEBS Lett* 583:499–505

Sonnenberg A, Liem RK (2007) Plakins in development and disease. *Exp Cell Res* 313:2189–203

Stinco G, Codutti R, Scarbolo M *et al.* (2005) A retrospective epidemiological study on the association of bullous pemphigoid and neurological diseases. *Acta Derm Venereol* 85:136–9

Young KG, Kothary R (2007) Dystonin/Bpag1 – a link to what? *Cell Motil Cytoskel* 64:897–905

Young KG, Kothary R (2009) Dystonin/Bpag1 is a necessary endoplasmic reticulum/nuclear envelope protein in sensory neurons. *Exp Cell Res* 314:2750–61